Influence of Base Frame/Slab Stiffness on Seismic Loading of Hybrid Isolation Systems

K.L. Ryan

Civil and Environmental Engineering, University of Nevada, Reno, Nevada, USA.

C.B. Coria

Dynamic Isolation Systems, McCarran, Nevada, USA.

2017 NZSEE Conference

ABSTRACT: Hybrid systems consisting of elastomeric bearings and sliders are widely used in practice. A full-scale 5-story steel moment frame building seismically isolated by a hybrid system of lead-rubber (LR) bearings and low friction roller bearings known as cross-linear (CL) bearings was tested at E-Defense in 2011. Although hybrid configurations of isolators help achieve desired stiffness and system stability, in this system a net transfer of axial force from LR bearings to CL bearings at large displacements was observed, because the out-of-plane rigidity of the base framing constrained the natural downward movement of LR bearings as they deformed laterally. In some cases, this constraint produced tension demands in the LR bearings. A numerical model of the test specimen was developed that was shown to reproduce the effects observed in the experiment, and a simplified model of the specimen was developed to explore the influence of base frame/slab stiffness on the axial force transfer. Preliminary results suggest that in buildings where the base slab stiffness is the same order as a typical floor slab, axial forces will distribute to the bearings more evenly under gravity loading, and the axial force transfer effects under lateral displacements will be more limited, such that the bearings are unlikely to experience net tension.

1 INTRODUCTION

The effectiveness of seismic isolation systems has been validated in prior earthquakes and through shake table testing, but field observations have generally been limited to intensities below the design level and shake table tests have generally used reduced scale specimens. To address the need for larger scale validation at large intensities, a full-scale 5-story base-isolated steel moment frame building was subjected to a series of earthquake excitations using the E-Defense shake table in Miki, Japan in August, 2011. A building specimen designed for a previous experiment was reconfigured with base isolation for this experiment. One configuration featured lead-rubber (LR) bearings, which are commonly used in isolation systems around the world. The isolation system was designed based on the seismicity of a potential site in Eastern US. To overcome design constraints frequently encountered in lightweight buildings, the isolation system paired the LR bearings with low friction rolling bearings known as cross-linear (CL) bearings. The CL bearings are tension capable rolling bearings with negligible horizontal resistance that have the potential to stabilize the isolation systems at large displacements and resist tensile loads induced by overturning. However, the CL bearings are vertically stiffer than the LR bearings, and do not displace downward at large horizontal displacements, which introduces a displacement incompatibility between the two types of bearings in the deformed configuration. Nevertheless, hybrid systems consisting of elastomeric bearings and sliding or rolling bearings are widely used in practice, with applications in New Zealand, Japan, Italy, Korea and China (Higashino and Okamoto 2006, Pan et al. 2005).

Throughout the test program, a net transfer of axial force from LR bearings to CL bearings was observed, because the out-of-plane rigidity of the base framing constrained the natural downward movement of LR bearings as they deform laterally. The axial force transfer increased as the bearing lateral displacement increased, and in some cases produced tension demands in the LR bearings. A numerical model of the E-Defense building test specimen, which features a multi-spring bearing model to account

for the bearing lateral-vertical interaction, has been developed and calibrated to represent the experimental results (Coria et al. 2015).

The axial force transfer effect in the experiment is believed to have been exaggerated by the presence of a stiff base slab that was designed to affix the building rigidly to the shake table (for testing in the non-isolated configuration). Theoretically, the flexibility of a typical floor slab can absorb some of the lack of compliance in the bearing vertical displacement through flexure, especially as the span between the bearings increases. Nonetheless, the experimental observations suggest potential limits at which hybrid systems can sensibly be applied. Most LR bearing models used in practice do not account for the shortening and reduction in vertical stiffness as a function of axial displacement, and practical guidance is needed for engineers to account for this issue in design.

The objective of this paper is to evaluate the influence of base slab stiffness on the axial force transfer effect. The effects of axial force transfer in the E-Defense test are presented and interpreted. A simplified version of the E-Defense building model, using the same multi-spring bearing model, is developed. The flexibility of the base slab in the simplified building model is varied, and the influence of this slab flexibility on the axial force transfer is evaluated.

2 E-DEFENSE TEST OBSERVATIONS

2.1 Building Specimen and Isolation System

The building specimen used in the test program was a two-bay by two-bay five-story steel moment frame building, 16 m tall and 12 m by 10 m in plan (Fig. 1). Floors 2-6 had fully composite concrete slabs connected to steel beams via shear studs. Effective "live load" with supplemental concrete blocks on Floors 2-5 (Fig. 1(b)), and supplemental steel plates bolted to one side of the roof. The estimated weight of the building based on self-weight of all the components was 5122 kN, while the actual weight measured by the cranes prior to placing the specimen was 5220 kN. The building specimen was designed to be fixed to the shake table through the base framing shown in Figure 2(a). The column base connected to stiffened steel boxes with dimensions of 2.5 m square by 0.9 m high. The base frame between the boxes consisted of 0.9 m deep girders and diagonal bracing.

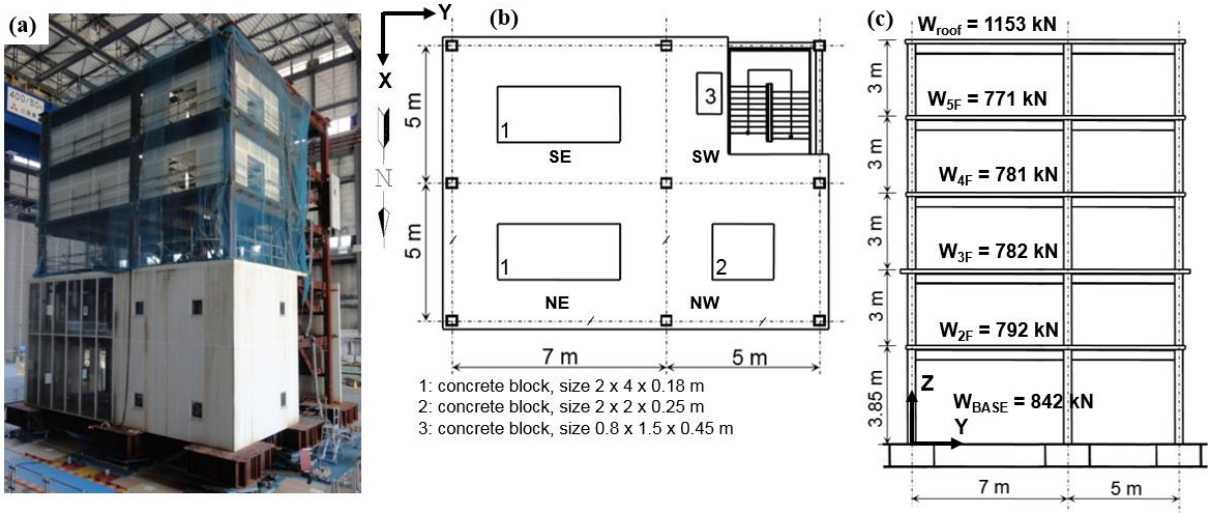

Figure 1: Test building (a) photo, (b) typical floor plan, and (c) elevation view with total weight per floor

The isolation system was designed with consideration of a very rare earthquake (return period of 100,000 years) at the Vogtle site in Eastern U.S., comparable to a typical design earthquake for many locations on the U.S. west coast. The response of the system to the 10,000 year return period at Diablo Canyon site in Western U.S. was also of interest. Spectrum-matched motions for the Vogtle site (Huang et al. 2009) were used to evaluate isolator displacement demands for different values of characteristic strength (Q_d) and post-yield stiffness (K_d). Preliminary design parameters were selected to target a displacement demand of 600 mm; the system provided actual post-yield period T_d = 2.84 sec and characterized strength normalized by weight Q_d/W = 0.050.

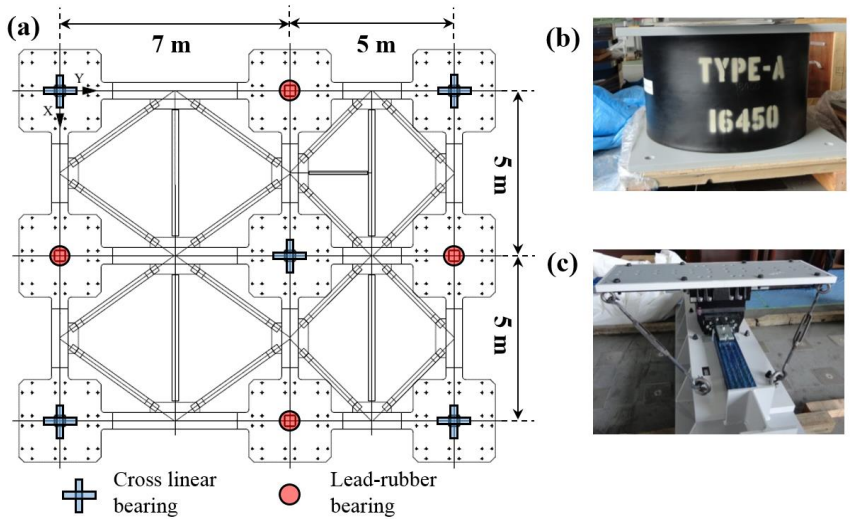

Figure 2: (a) Base framing and column box stiffeners with bearing locations superimposed; photo of (b) LR and (c) CL bearing

Four LR bearings and five CL bearings were placed as shown in Figure 2(a). The LR bearings (Fig. 2(b)) consisted of 40 alternating layers of elastomer and steel, a central lead plug, and steel plates at the top and bottom of the bearing. The basic dimensions of the LR bearing were: overall diameter D = 698.5 mm; bonded diameter D_b = 673.1 mm; lead plug diameter D_p = 101.6 mm; steel shim thickness t_s = 3.0 mm; and rubber layers thickness t_r = 6.0 mm. The design properties of the bearing were: elastic stiffness K_1 = 6.5 kN/mm, post-yield stiffness K_{do} = 0.65 kN/mm, characteristic strength Q_{do} = 65.7 kN, which led to yield force F_y = 73 kN, yield displacement D_y = 11.28 mm, and vertical stiffness in compression of 1500 kN/mm. The CL bearings (Fig. 2(c)) were composed of two sets of perpendicular rails with top and bottom guided plates separated by nearly frictionless ball bearings. The bearings allowed free movement in any horizontal direction with a coefficient of friction in the range of 0.48-0.62%. The vertical stiffnesses were provided by the manufacturer and determined from theoretical calculations as: 3471 kN/mm in compression and 245 kN/mm in tension. Safety stops were installed at the end of the CL bearing rails to prevent displacement exceeding +/- 600 mm and to thereby prevent shear rupture or instability of LR bearings.

2.2 Observations of Axial Load Transfer during the Test

Bearing axial force variation as a function of time was observed in all motions. Different factors contributed to the axial force variation such as initial load distribution, overturning, shift in mass centre, vertical excitation, and force transfer between the LR bearings and CL bearings. The last effect is caused by the out-of-plane rigidity of the base framing and the discrepancy in the vertical stiffness of the LR and CL bearings. Normally, when an LR bearing is subjected to compression and is laterally displaced, the bearing reduces in height (Fig. 3(a)). However, for the hybrid system, the free shortening of the LR bearing is prevented by the vertical stiffness of the CL bearing and the base framing. As a result, a portion of the axial force ΔP is redistributed, causing the axial force to decrease in the LR bearing and increase in the CL bearing (Fig. 3(b)). This device force transfer is distinct from and unrelated to dynamic force variation due to overturning effects. If the force transferred (ΔP) exceeds the bearing force (P_{LR}), individual bearings may sustain tension.

Evidence of device force transfer was observed during the test program. Histories of isolator displacements and axial forces on individual LR bearings and summed over all LR bearings are shown for two imposed input excitations: a multi-cycle sine wave called SIN100(Y)-1 (Fig. 4(a)), and 95% of an XY motion spectrum matched to the site-specific design spectrum for the Diablo Canyon site called DIA95(XY) (Fig. 4(b)). In SIN100(Y)-1, vertical lines drawn through local peaks of the vector sum displacements and extended down through the axial load highlight the instantaneous responses at these peaks. At each instant of a local maximum or minimum displacement, a corresponding net reduction in total axial force of the 4 LR bearings was observed. The axial forces in individual LR bearings were more complex since overturning effects were present. The N and S bearings, being located close to the centre of the building plan for Y-direction shaking, did not experience much overturning, but were subjected to some unloading at every local displacement peak. The E and W bearings showed evidence of overturning induced axial force variation, wherein the compressive force was near a local maximum for the W bearing and a local minimum for the E bearing at positive Y-direction peak displacements. This trend was reversed for negative Y-direction peak displacements. Thus, for this excitation,

overturning-induced axial force variation in the E and W bearings was dominant, but device force transfer also contributed to the total axial force variation.

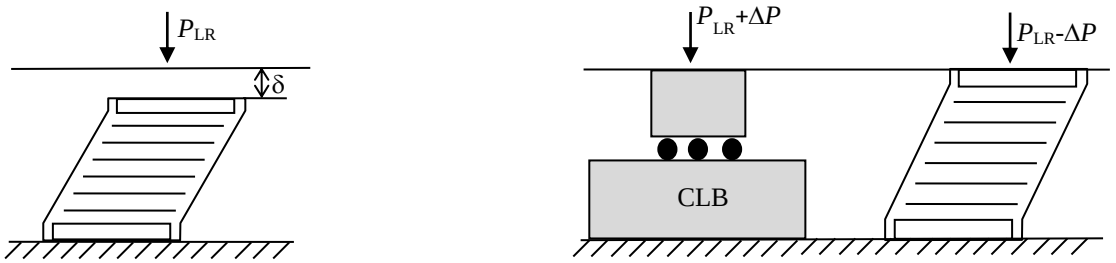

(a) LR bearing with shortening (δ) (b) CL bearing and LR bearing without shortening

Figure 3: Resultant action on LR bearing as a result of CL bearing and base framing constraint

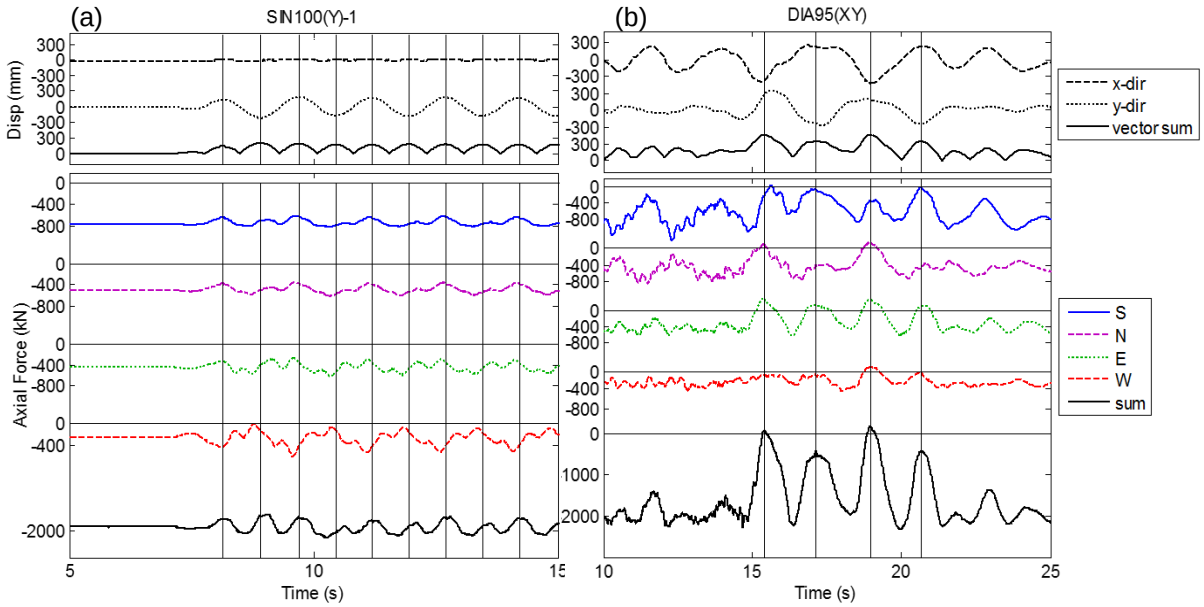

Figure 4: History of average horizontal displacement (x, y and vector sum), and axial force in individual LR bearings and summed over all LR bearings for (a) SIN100(Y)-1 and (b) DIA95(XY).

For DIA95(XY) (Fig. 4(b)), substantial device force transfer, as indicated by axial unloading of each individual LR bearing, occurred 4 times corresponding to instantaneous local peaks of the vector sum displacement at the building centre. The E bearing sustained tension at every local displacement peak, and for two of the peaks (occurring just after 15 sec and at about 19 sec), the total axial load on the LR bearings exceeded 0, indicating that the entire weight of the building had shifted to the CL bearings. This device load transfer was much more significant for DIA95(XY) than for SIN100(Y)-1 since the isolator displacement was much larger (550 mm compared to 210 mm).

2.3 **Numerical Predictions of Axial Force Transfer**

A computational model of the building and isolation system was developed in OpenSees to simulate the seismic response observed during the experiments. Each LR bearing was represented by a multiple spring model that accounts for the bearing lateral-vertical interaction. The multi-spring model, based on the works of Yamamoto et al. (2009) and Han et al. (2014), sandwiches elastic shear springs between two layers of distributed axial springs (Fig. 5(a)). The shear spring properties were applied to corotational truss elements that allow for rotation of the springs within the bearing, thus accounting for the interaction between the bearing shear and axial response. The planar spring assemblage that includes pairs of shear springs connected to the outer axial springs by rigid elements was replicated at equally spaced angles about a vertical axis to achieve comparable stiffness in two lateral directions (Fig. 5(b)). The entire distributed spring model is in parallel with a nonlinear bidirectionally coupled elastic-plastic

spring that represents the energy dissipation of the lead core (Fig. 5(a)). For further details about the theory and implementation of the model, refer to Coria et al. (2015).

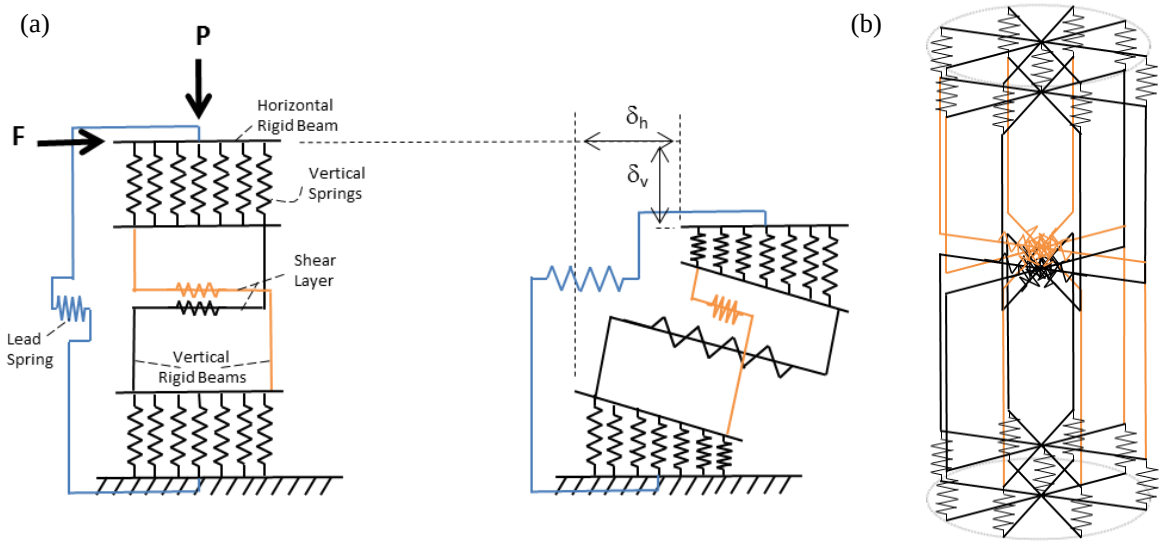

Figure 5: (a) Planar depiction of multi-spring model in undeformed and deformed configurations and (b) 3D depiction of multi-spring model with shear spring pairs replicated every 45º around the vertical axis

The model shear spring properties were assigned to represent the design post-yield stiffness K_{do}, while the elastic-plastic spring represented the characteristic strength Q_{do}. The total vertical stiffness of the linear axial springs was reduced to k_{vo} = 1000 kN/mm to account for flexibility of load cell assemblies present beneath the bearings during the tests. Two model configurations were considered: the first with two planar assemblages in orthogonal directions (MS2) and the second with four planar assemblages separated by 45 degree angles (MS4), which is reflected in Fig. 5(b). The axial spring stiffnesses were selected as follows: MS2, centre spring = $1.5k_{vo}$, and four exterior springs = $0.125k_{vo}$ each; MS4, centre spring = $1.5k_{vo}$ and eight exterior springs = $0.0625k_{vo}$. The spring stiffnesses are based on tributary area; note that total stiffness of each layer is $2k_{vo}$ since the axial spring layers are combined in series. A lateral-vertical uncoupled bearing model was considered for reference.

Figures 6 and 7 compare the numerically simulated and experimentally observed total axial force histories for SIN100(Y)-1 and DIA95(XY), respectively. For SIN 100(Y)-1, the axial force transfer (evidenced by net reduction in total LR bearing axial force at instances corresponding to displacement peaks) is captured well by both the MS2 and MS4 LR bearing models (Figs. 6(b) and (c)). For DIA95(XY), the MS2 and MS4 bearing models reflect some load transfer, but not as much as was observed in the experiment (Figs. 7(b) and 7(c)). Since the extent of force transfer increases nonlinearly with displacement amplitude, the shortfall is partly because the bearing peak lateral displacements were underestimated by the bearing model (not shown here). No significant differences are observed between the MS2 and MS4 configuration. The uncoupled bearing model does not capture the axial force transfer at all for either motion (Figs. 6(a) and 7(a)).

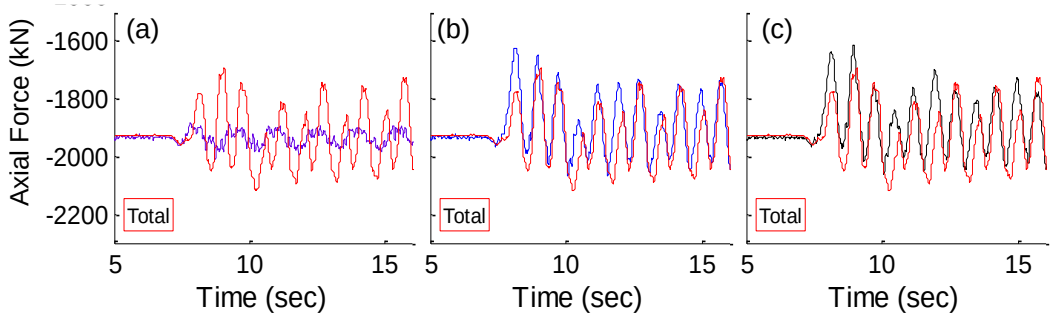

Figure 6: Experimental (red) and numerically simulated total axial force in LR bearings for SIN100(Y)-1, using (a) uncoupled, (b) MS2, and (c) MS4 LR bearing models.

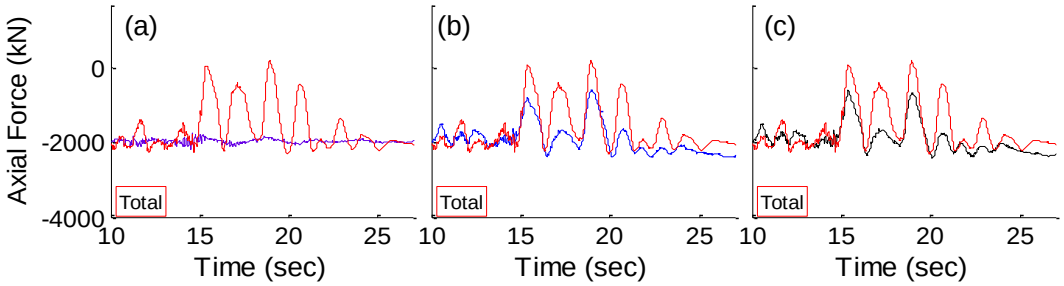

Figure 7: Experimental (red) and numerically simulated total axial force in LR bearings for DIA95(XY) using (a) uncoupled, (b) MS2, and (c) MS4 LR bearing models.

3 INFLUENCE OF BASE FRAME STIFFNESS ON AXIAL FORCE TRANSFER

3.1 Simplified Single Story Building Model

To investigate the influence of base frame stiffness on the axial force transfer, a simplified single story building model based on the E-Defense specimen was developed. The model is conceptually shown in Figure 8. The plan dimensions are 14 m x 10 m, with symmetric two-bay frames in each direction. The story height is 4 m. Like the test specimen, the model incorporates LR bearings at the edge columns, and CL bearings at the centre and corner columns. LR bearings are modelled using MS2 as described in Section 2.3, except the vertical stiffness was assigned as the theoretical value k_{vo} = 1500 kN/mm. CL bearings are modelled with a bidirectionally coupled elastic-perfectly plastic spring to represent lateral force-deformation, and a bilinear elastic spring in the vertical direction to represent the nominal vertical stiffness in tension and compression (Section 2.1). The single story building was modelled with generic steel sections applied to linear frame elements and centreline moment connections. For consistent isolation system dynamic properties, the total E-Defense specimen weight =5250 kN (and equivalent mass) was uniformly distributed over all beams: 1/5 at the base level and 4/5 at the first story level. The same section was applied to all columns and first story beams, and its moment of inertia was calibrated so the fundamental period of the frame in the fixed-base condition was 0.4 sec. Rayleigh damping was assigned to the superstructure, calibrated to a damping ratio of 0.025 at the isolation frequency (T = 2.84 sec) and the first mode structural frequency (T = 0.4 sec).

Five different values were selected for the moment of inertia of base girders: I = 0.001, 0.01, 0.1, 0.6 and 6 m^4. The smallest value (I = 0.001 m^4) is on the order of magnitude of the effective I – including the composite effects of the concrete floor slabs - of the test specimen 2nd floor, which ranged from 0.003 to 0.005 m^4. The fourth value (I = 0.6 m^4) is comparable to the effective I of the test specimen base girder, with an adjustment for the shortened length of the frame members due to the columns stiffeners. The largest value (I = 6.0 m^4) is an order of magnitude higher than the test specimen, and thus essentially rigid.

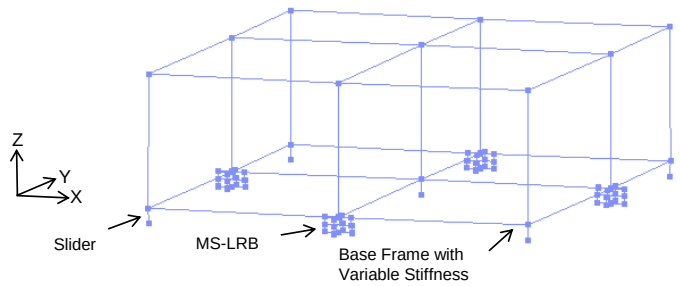

Figure 8: Concept sketch of single-story building model

3.2 Simulation Results

First, each model was subjected to a gravity analysis followed by a cyclic pushover analysis (single cycle with lateral displacement amplitude of 400 mm in the Y, or E-W direction). Figure 9 shows the lateral displacement loading, the total axial force summed over the LR bearings normalized by the weight W of the building, and the vertical displacement versus lateral displacement of the North (N) bearing. For the most flexible base girders, about half of the building weight is distributed to the LR bearings under the initial gravity analysis, which is in accordance with the tributary area (Fig. 9(b)). However, as the base girders become stiffer, an increasingly smaller portion of the building weight is carried by the LR

bearings (around 0.2*W* for rigid base girders Furthermore, for the most flexible girders, the bearings are less constrained to move downward under a lateral displacement (Fig. 9(c)), and thus the axial load transfer from the LR to the CL bearings is moderate (around 0.15*W* in Fig. 9(b)). Under increasing base girder stiffness, the constraint on downward movement of the bearing increases, and the axial load transfer increases (around 0.3*W* for rigid base girders). Thus, the model predicts that the LR bearings will experience net tension for the stiffest two base girder cases (I = 0.6 and 6 m^4). However, this model may overestimate tensile forces in the LR bearings, since individual axial springs were modelled as linear and do not account for the tension yielding that will occur over portions of the bearing as it unloads.

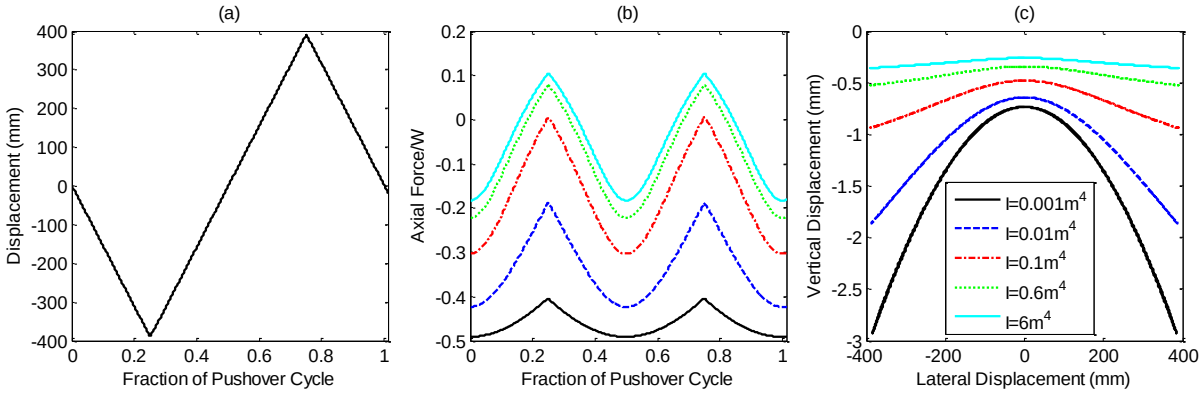

Figure 9: Numerically simulated cyclic pushover for single story model with variable base girder stiffness: (a) displacement history, (b) normalized total LR bearing axial force, and (c) vertical displacement vs. lateral displacement

Figure 10 demonstrates vertical displacement and axial force variations in individual LR bearings for flexible and stiff base girders. The responses in N and S bearings were identical. The differences in individual bearings are modest compared to overall differences imposed by base girder flexibility. For the flexible base girder case (Fig. 10(a)), the axial force unloading pattern reflects the effects of overturning (i.e. the compression side bearing unloads less than the tension side bearing). For the stiff base girder, the axial force transfer effect is dominant compared to overturning (Fig. 10(b)).

Figure 11 shows the absolute displacement of the N bearing, and normalized total and relative axial force in LR bearings under DIA95(X) ground motion input. As expected, instances of maximum axial force unloading are aligned with peak lateral displacements. The bearing displacement is insensitive to the base girder stiffness (Fig. 11(a)), but again increased base girder stiffness causes LR bearings to carry less of the building weight under static loading, and a greater axial force transfer effect leading to net tension in the bearings (Fig. 11(b)). The relative axial force transfer (Fig. 11(c)) – computed from total minus static axial force – suggests that the relative axial force transfer approaches an upper limit with increasing base girder stiffness.

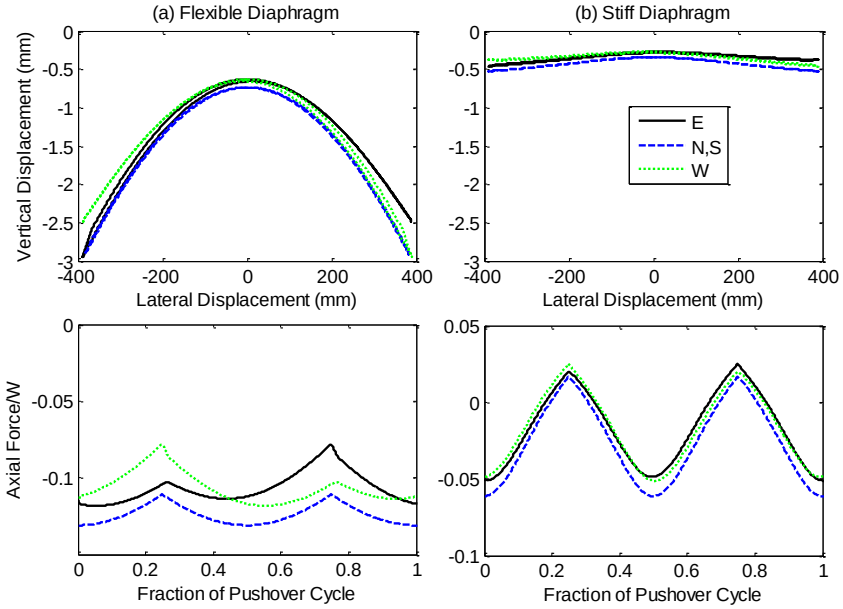

Figure 10: Vertical displacement and axial force in individual LR bearings under cyclic pushover analysis for (a) flexible base girder (I = 0.001 m^4)and (b) stiff base girder (I = 0.6 m^4)

4 CONCLUSIONS

In an experimental study of a hybrid isolation system combining LR bearings and rolling CL bearings, a significant transfer of axial forces from LR bearings to CL bearings at large lateral displacements was observed, which resulted in net tension to the LR bearings in some simulations. These observations, which have been reproduced numerically, have raised concerns about the suitability of hybrid isolation systems incorporating devices with different vertical stiffnesses. However, the axial load transfer in the experiment may have been exaggerated due to the very stiff base girder.

A simplified model of the specimen was developed to explore the influence of base frame/slab stiffness on the axial force transfer. These preliminary results suggest that in buildings where the base slab stiffness is the same order as a typical floor, axial forces will distribute to the bearings more evenly under gravity loading, and the axial force transfer effects will be more limited, such that the bearings are unlikely to experience net tension. Engineers wishing to use hybrid systems should proceed cautiously with careful consideration of the possible base slab effects; very stiff base slabs should be avoided. These conclusions are preliminary as tensile yielding of the bearings and flexural demands on the base slabs should be more carefully considered.

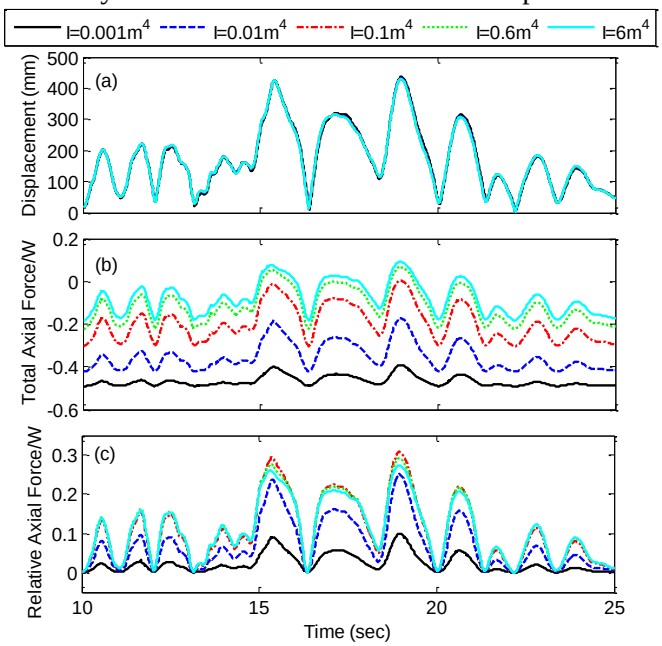

Figure 11: Single story model with variable base girder subjected to DIA95(XY): (a) displacement amplitude of N bearing; normalized (b) total and (c) relative LR bearing axial force

5 ACKNOWLEDGMENT

This project was based on work under the primary sponsorship of the U.S. Nuclear Regulatory Commission through Contract NRC-HQ-11-C-04-0067, and a larger collaboration between the National Science Foundation (NSF) through Grant CMMI-1113275 and Japan's National Research Institute for Earth Science and Disaster Prevention (NIED). Financial support, product donations and in-kind technical support were provided by Dynamic Isolation Systems and Aseismic Devices Company. The authors are grateful for all contributions that led to the success of this project. Any opinions, findings, and conclusions or recommendations expressed in this material are those of the authors alone and do not necessarily reflect the views of the sponsors.

6 REFERENCES

Coria, C.B., Ryan, K.L., Dao, N.D. 2015. Response of lead-rubber bearings in a hybrid isolation system during a large scale shaking experiment of an isolated building, *CCEER Report 15-9*, Center for Civil Earthquake Engineering Research, University of Nevada, Reno, NV, USA, 2015.

Han, X., Warn G. 2014. Mechanistic model for simulating critical behavior in elastomeric bearings, *J. Struct. Eng.*, 10.1061/(ASCE)ST.1943-541X.0001084.

Higashino, M., Okamoto, S. 2006. *Response Control and Seismic Isolation of Buildings (CIB Proceedings)*, Taylor & Francis, 1st Edition.

Pan, P., Zamfirescu, D., Nakashima, M., Nakayasu, N., Kashiwa, H. 2005. Base-isolation design practice in Japan: Introduction to the post-Kobe approach. *J. Earthq. Eng.*, 9(1):147-171.

Yamamoto, S., Kikuchi, M., Ueda, M., Aiken, I.D. 2009. A mechanical model for elastomeric seismic isolation bearings including the influence of axial load, *Earthq. Eng. Struct. Dyn.*, 38:157–180.